PROCEEDINGS OF SPIE

SPIEDigitalLibrary.org/conference-proceedings-of-spie

Improved optical enhancement in binary plasmonic gratings with nanogap spacing

Ahmad Darweesh, Stephen Bauman, Zachary Brawley, Joseph Herzog

Ahmad A. Darweesh, Stephen J. Bauman, Zachary T. Brawley, Joseph B. Herzog, "Improved optical enhancement in binary plasmonic gratings with nanogap spacing," Proc. SPIE 9927, Nanoengineering: Fabrication, Properties, Optics, and Devices XIII, 99270Z (15 September 2016); doi: 10.1117/12.2237197



Event: SPIE Nanoscience + Engineering, 2016, San Diego, California, United States

Improved optical enhancement in binary plasmonic gratings with nanogap spacing

Ahmad A. Darweesh^a, Stephen J. Bauman^a, Zachary T. Brawley^b, Joseph B. Herzog ^{a,b}

^aMicroelectronics-Photonics Program, University of Arkansas, Fayetteville, AR, 72701, USA; ^bDepartment of Physics, University of Arkansas, Fayetteville, AR, 72701, USA;

ABSTRACT

This work thoroughly investigates binary nanowire gratings with nanogap spacing. A binary plasmonic grating is a periodic nanostructure for which each period has two different widths. The study has determined that plasmonic gratings with two different widths in each period give rise to optical enhancement that is 2.1 times stronger than that of standard plasmonic grating structures. A map of varying width ratios has been created to illustrate the key geometric characteristic for enhancement optimization. The structure under investigation was a gold structure with a constant height of 15 nm and a nanogap of 5 nm. The period size of the structure depends on the two nanowire widths in each grating period. The optical enhancement $(E/E_0)^2$ of the geometry was investigated using a finite element method (FEM) simulation for various wavelengths. The results show a strong correlation between the plasmon wavelength and the periodicity of the gratings. Additionally, the plasmonic charge distributions have been calculated for various periods and geometries. Various resonant modes exist for the charge distribution, significantly affecting the enhancement depending on the nanowire widths.

Keywords: Plasmon, nanogap, Raman, plasmonic enhancement, SERS.

1. INTRODUCTION

Nano-optics is an important field that investigates nanoscale photonic materials; and it has been continuing to grow over the last two decades. It deals with structures that have dimensions smaller than the wavelength of light specifically between 1 and 100 nm. The collective oscillation of electrons in a piece of metal is called a plasmon. Some metallic nanostructures, such as nanowires, are capable of enhancing and confining electromagnetic fields due to the plasmonic excitation that generates on the metal's surface. The incident light can oscillate the charge distribution on the surface of nano-structures. As a result, the nano-structures can produce a net increase in the value of the local electric field. This is known as the optical enhancement, which is defined as the ratio between local electric field, and incident field all squared, $(E/E_0)^2$. ^{1, 2}

A horizontal one-dimensional periodic array of metallic nano-structures on a substrate separated by dielectric is called a plasmonic grating. Experimental and theoretical research have confirmed that not only can these nano-structures enhance the electric field, but using nanogaps that separate them can provide additional enhancement.³⁻⁶ "Hotspots" can be created via nanogap structures multiplying the magnitude of the electric field due to the plasmonic coupling between adjacent nano-structures. These hotspots can be harnessed for surface-enhanced Raman spectroscopy (SERS). Increasing the detection sensitivity of different chemical agents, even to the point of single molecule detection.⁷⁻¹⁰ Moreover, plasmonic enhancement can be utilized in a variety of different applications such as photovoltaics¹¹⁻¹⁸ and detection and diagnostics in biomedical fields (biosensing).¹⁹⁻²⁵ These types of applications use the plasmonic effects that generate from nanoparticle structures to strengthen the electrical or/and optical signals. Another significant application of plasmonic enhancement is to improve the efficiency of photo-detectors. For example, optimizing the nano-gaps between interdigital nano-electrodes of metal-semiconductor-metal photo-detectors based on semi-insulating GaAs can play an important role in enhancing photo-current via plasmonic effects.²⁶

Nanoengineering: Fabrication, Properties, Optics, and Devices XIII, edited by Eva M. Campo, Elizabeth A. Dobisz, Louay A. Eldada, Proc. of SPIE Vol. 9927, 99270Z ⋅ © 2016 SPIE CCC code: 0277-786X/16/\$18 ⋅ doi: 10.1117/12.2237197

2. DUAL WIDTH MODEL

A binary width periodic nanostructure (dual width plasmonic structure) consists of two different slab widths that are separated by a nanogap. Fig. 1(a) displays the cross-sectional view of a single period (P) of binary nanostructures that have various gold widths (w_1 and w_2) with 15 nm of fixed thickness (the height of gold nanowires). The top edges of the nanowires are beveled by simulating a fillet of 4 nm to provide a closer approximation to an actual nanowire fabricated with electron beam lithography (EBL). The nanowires are separated by a gap width of s = 5 nm. To study the precise effects of dual width plasmonic gratings, the widths of gold nanowires were swept through different ranges. For SERS applications, an effective medium approximation ($n_{\rm eff} = 1.25$), which represents the average refractive indices of air and SiO₂ surrounding the nanowires, is used. To generate a finite array of the nanostructures in the x-direction, a periodic condition is applied to the left and right sides of the model. The incident light of different wavelengths (λ) is simulated to hit the nanowire surface with normal incidence the top of the space (k). The electric field (E_0) of the incident light is polarized in the direction of periodicity. The top and bottom of the model have perfectly matched layers (PMLs), which are used to absorb the scattered light so that it does not affect calculations. The model was conducted by using finite element method (FEM) simulations (COMSOL 5.0) in order to calculate the optical enhancement that resulted from the binary width plasmonic gratings in the gap.

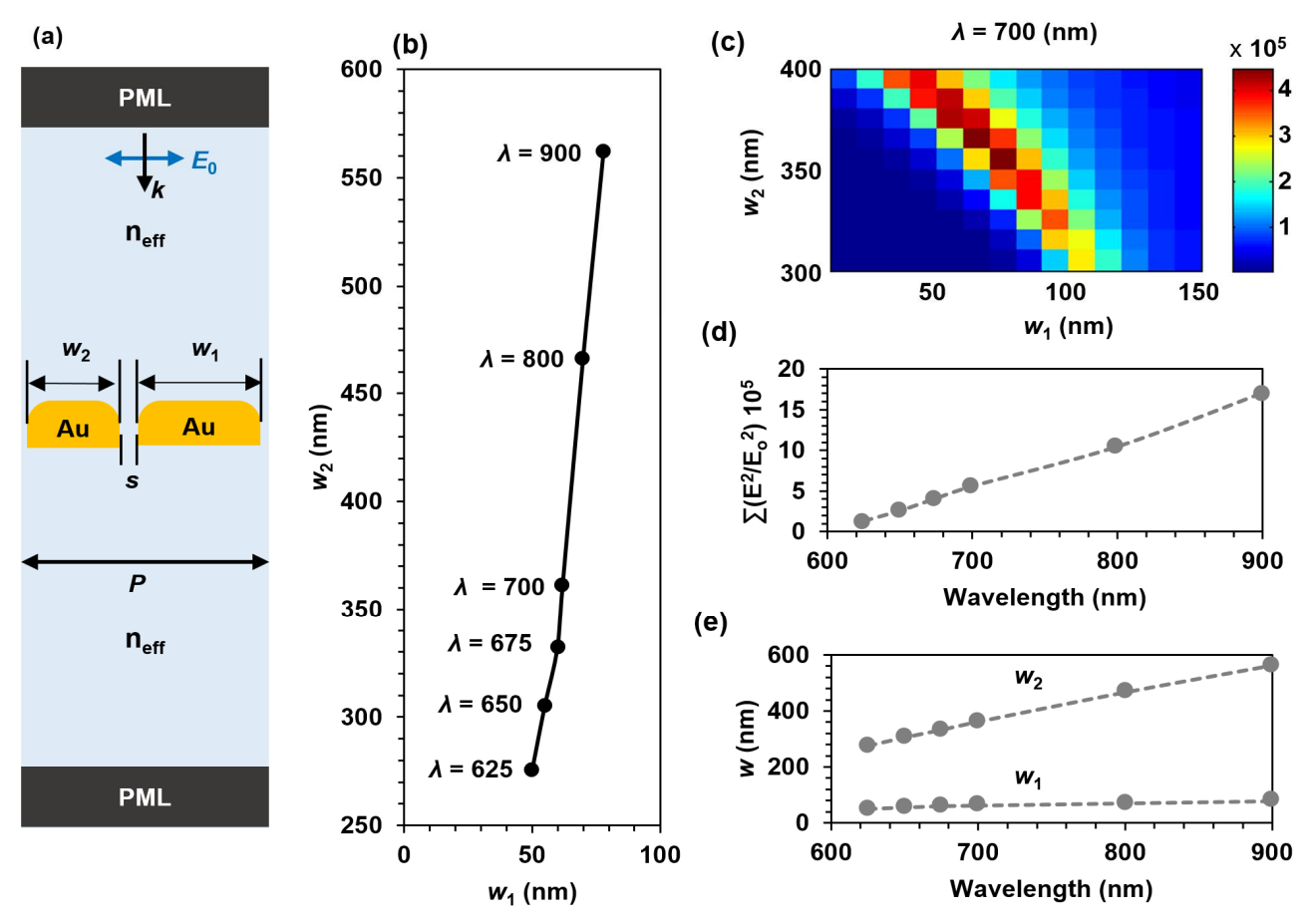


Figure 1. (a) Cross-sectional simulation space depiction containing the dual plasmonic grating of Au nanowires with 15 nm thickness. The following parameters are indicated: the incident light direction (k), direction of polarization (E), single period of the grating (P), perfectly matched layers (PMLs), effective medium (n_{eff}) , structures $(w_1 \text{ and } w_2)$, and gap width (s). Periodic boundary conditions were applied in both horizontal directions. (b) Simulation results that plot the dual width geometry $(w_1 \text{ and } w_2)$ which gives the maximum optical enhancement at different wavelengths. (c) Maximum optical enhancement as a function of nanowire widths $(w_1 \text{ and } w_2)$ for dual width grating for 700 nm wavelength incident light. (d) Plot of maximum optical enhancement vs different wavelengths. (e) Shows the correlation between nanowire widths as a function of wavelength at maximum optical enhancement.

Fig. 1(b) shows the plot of the linear relationship between w_1 and w_2 that were swept through different ranges. It displays that increasing the wavelength can increase the maximum optical enhancement at the gap space. By using this plot, it is possible to determine the optimal nanowire widths when a particular wavelength is used. In addition, it is possible to

determine the maximum optical enhancement for a combination of w_1 , w_2 , and wavelength, as needed. The color map of maximum optical enhancement as a function of w_1 and w_2 is plotted in Fig. 1(c) for an incident wavelength of 700 nm. It reveals that the maximum optical enhancement, which is represented by dark red spot, was 4.5 x 10⁵ when $w_1 = 60$ nm and $w_2 = 360$ nm. The plot in Fig. 1(d) shows that the summation of optical enhancement is directly proportional to the wavelength of incident light. Plus, this plot can give an estimated number of maximum optical enhancement at any particular wavelength. Two equations have been derived from the two linear relationships that appear in Fig. 1(e). The first equation, $w_1 = 0.095\lambda - 6.4$ (nm), shows the correlation between w_1 and the wavelength, whereas the second equation, $w_2 = 1.04\lambda - 372$ (nm), shows the relationship between w_2 and the wavelength. From these equations one can calculate the optimal values of w_1 , w_2 , and the period of the structure at a particular wavelength.

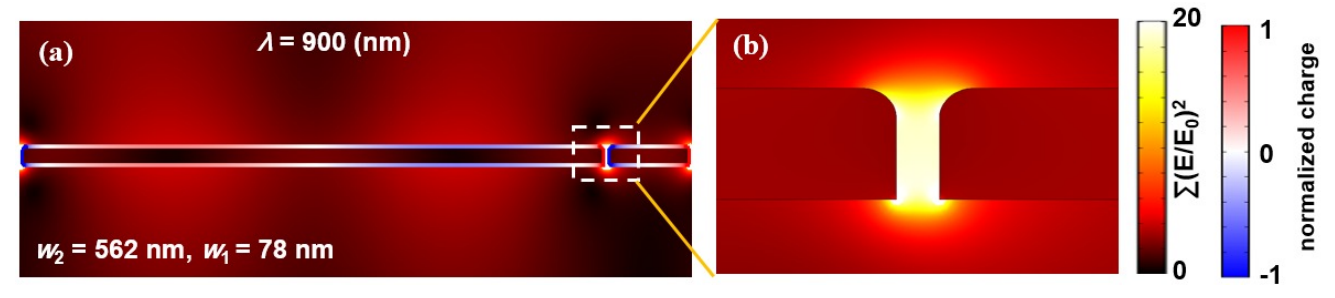


Figure 2. (a) Simulation results of a cross section of the entire periodic structure that includes $w_1 = 78$ nm, $w_2 = 562$ nm, and s = 5 nm. It shows electric field and charge distribution when the wavelength of incident light $\lambda = 900$ nm. The normalized charge distribution and electric field enhancement $(E/E_0)^2$ are indicated by color bars. (b) Represents the enlarged dashed square, in (a), that contains the edges of w_1 and w_2 , and the whole gap width (s). The widths in this model are the sizes that give the maximum enhancement in the gap for 900 nm light. The model is simulated by using an effective medium, $n_{\text{eff}} = 1.25$, surrounding the Au nanowires.

Fig. 2. Shows the enhanced electric field and charge distributions of the structure when $w_1 = 78$ nm, $w_2 = 562$ nm, $n_{\rm eff} = 1.25$, and the incident light wavelength $\lambda = 900$ nm. In Fig. 2(a), since the width of each nanowire is different, it is obvious that the enhanced charge distribution for both nanowires are completely different as well. Although the charges are massed at the nanowire edges, one can see that w_2 supports a plasmon with 4 anti-nodes, whereas w_1 supports dipolar resonance due to the difference in nanowire widths. Fig. 2(b) is the enlarged dashed square in (a) that includes the edges of the two nanowires and gaps (s = 5 nm); it displays the enhanced electric field distribution. Depending on the charge distribution, which in turn depends on the nanowire widths, the optical enhancement $(E/E_0)^2$ can increase or decrease. The coupling between the charges at the edges of the nanowires increases the optical enhancement when the nanowire widths are different because the dual-width structure can create a hybridized grating plasmon between them _one of the benefits of dual-width gratings.^{28, 31-33}

3. STANDARD GRATING ON GaAs

Using the results from above, next we focus on a plasmonically enhanced GaAs photo-detector application. Here we define the standard grating as a nanowire array which has nanowires that have the same widths for the entire grating. Fig. 3(a) displays a single grating structure that comprises the same elements as in Fig. 1(a). This model, however, includes air on the top of the structure and gallium arsenide (GaAs) beneath, instead of n_{eff} . In addition, the nanowire widths are equal ($w_1 = w_2 = w$) for this model. Fig. 3(b) plots the average optical enhancement in the GaAs, $(E/E_0)^2$, versus the nanowire width, w, for different gap widths. The average optical enhancement was calculated for only the GaAs substrate. In one instance, the nanowire width was swept from 10 nm to 500 nm with 10 nm of step size. Next, the gap width was swept from 5 nm to 50 nm. The simulated wavelength in this model was 875 nm, as this corresponds to the bandgap of the electrons in the GaAs substrate. The plot illustrates that increase the nanowire width can create an average optical enhancement curve with multiple-peaks. These peaks significantly decrease when the nanowire width increases. Moreover, the whole curve, including the peaks, decreases with increasing gap width. This behavior tells us that smaller gap widths can produce larger electric field enhancement, which means better optical enhancement. Increasing the nanowire width can cause each peak to red shift when the gap width increases, as shown in Fig. 3(c-d). These figures unfold that the difference between the peaks at the first peak (P_0) is extremely large, whereas the difference considerably decreases at the second peak (P_1) and the other peaks (P_2) , and (P_3) as well.

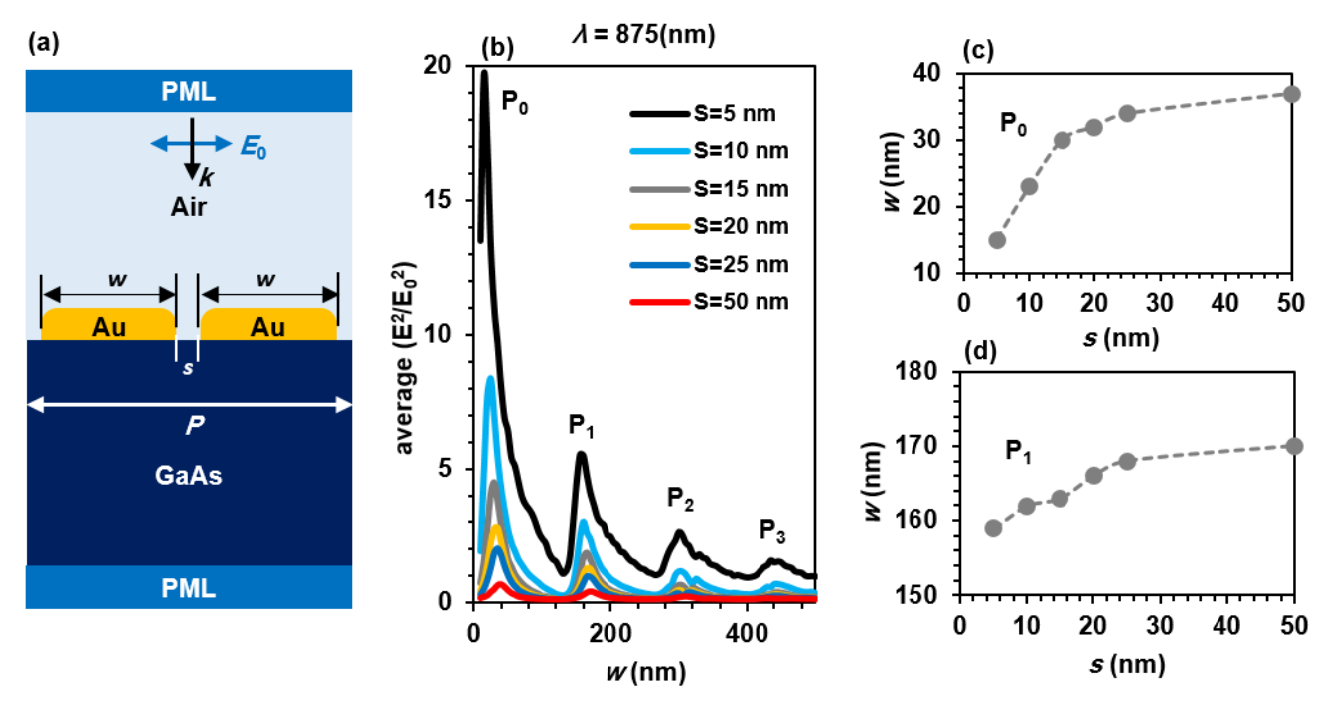


Figure 3. (a) The depiction of cross-sectional simulation space that involves the plasmonic grating of Au nanowires on a GaAs substrate with air above them. (b) Simulation results showing the relationship between the average optical enhancement Ave $(E/E_0)^2$ in the GaAs substrate and structure width, w, for different gap width, s, when the incident wavelength is $\lambda = 875$ nm. The plot shows different peaks when the nanowire width is increased. (c-d) Plots display the first and second peaks that appear in (b). The plots shows the relationship between nanowire width, w, with gap width, s.

The relationship between average optical enhancement and gap widths at (P_0) and (P_1) that appear in Fig. 3(b) are shown in Fig. 4.

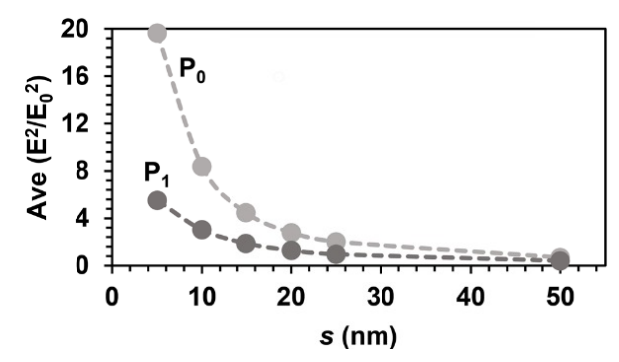


Figure 4. Plot showing the relationship between the average optical enhancement $(E/E_0)^2$ and gap width, s, for P_0 and P_1 that appear in figure 3b.

4. CONCLUSION AND FUTURE WORK

This work presents dual-width plasmonic gratings enhancement results and single gratings results on a GaAs substrate for photo-detectors. For the dual-width gratings, it is found that increasing the wavelength of incident light can increase the optical enhancement in the gaps. In addition, two linear equations have been derived that can be used to calculate the optimal structures and wavelength. On the other hand, a strong reverse relationship has been found between the optical enhancement in the GaAs substrate and the gaps that separate the nanowires for a single grating. Moreover, many peaks have been shown in the optical enhancement curve. The peaks can give an indication of the optimal structures. Dual-

width plasmonic gratings on GaAs will be future work of this project to find out the effect of various nanowire widths on the optical enhancement and the efficiency of photo-detectors.

REFERENCES

- [1] Bauman, Stephen J., Ahmad A. Darweesh, and Joseph B. Herzog. "Surface-enhanced Raman spectroscopy substrate fabricated via nanomasking technique for biological sensor applications." In SPIE OPTO, pp. 97591I-97591I. International Society for Optics and Photonics, 2016.
- [2] Thongrattanasiri, Sukosin, and F. Javier García de Abajo. "Optical field enhancement by strong plasmon interaction in graphene nanostructures." Physical review letters 110, no. 18: 187401 (2013).
- [3] Zhu, Wenqi, Mohamad G. Banaee, Dongxing Wang, Yizhuo Chu, and Kenneth B. Crozier. "Lithographically fabricated optical antennas with gaps well below 10 nm." Small 7, no. 13: 1761-1766 (2011).
- [4] Chen, Xiaoshu, Hyeong-Ryeol Park, Matthew Pelton, Xianji Piao, Nathan C. Lindquist, Hyungsoon Im, Yun Jung Kim et al. "Atomic layer lithography of wafer-scale nanogap arrays for extreme confinement of electromagnetic waves." Nature communications 4 (2013).
- [5] Chen, Xiaoshu, Cristian Ciraci, David R. Smith, and Sang-Hyun Oh. "Nanogap-enhanced infrared spectroscopy with template-stripped wafer-scale arrays of buried plasmonic cavities." Nano letters 15, no. 1: 107-113 (2014).
- [6] Lumdee, Chatdanai, Binfeng Yun, and Pieter G. Kik. "Gap-plasmon enhanced gold nanoparticle photoluminescence." Acs Photonics 1, no. 11: 1224-1230 (2014).
- [7] De Leebeeck, A., Kumar, L. K. S., de Lange, V., Sinton, D., Gordon, R., Brolo, A. G., "On-Chip Surface-Based Detection with Nanohole Arrays," Anal. Chem. 79(11), 4094–4100 (2007).
- [8] Gordon, R., Sinton, D., Brolo, A. G., Kavanagh, K. L., "Plasmonic sensors based on nano-holes: technology and integration," 2008, 695913–695913 6.
- [9] Eftekhari, F., Escobedo, C., Ferreira, J., Duan, X., Girotto, E. M., Brolo, A. G., Gordon, R., Sinton, D., "Nanoholes As Nanochannels: Flow-through Plasmonic Sensing," Anal. Chem. 81(11), 4308–4311 (2009).
- [10] Sonntag, M. D., Klingsporn, J. M., Zrimsek, A. B., Sharma, B., Ruvuna, L. K.., Van Duyne, R. P., "Molecular plasmonics for nanoscale spectroscopy," Chem Soc Rev 43(4), 1230–1247 (2014).
- [11] Catchpole, K. R., Polman, A., "Plasmonic solar cells," Opt. Express 16(26), 21793 (2008).
- [12] Nakayama, K., Tanabe, K., Atwater, H. A., "Plasmonic nanoparticle enhanced light absorption in GaAs solar cells," Appl. Phys. Lett. 93(12), 121904 (2008).
- [13] Atwater, H. A., Polman, A., "Plasmonics for improved photovoltaic devices," Nat. Mater. 9(3), 205–213 (2010).
- [14] Ferry, V. E., Verschuuren, M. A., Li, H. B. T., Verhagen, E., Walters, R. J., Schropp, R. E. I., Atwater, H. A., Polman, A., "Light trapping in ultrathin plasmonic solar cells," Opt. Express 18(S2), A237–A245 (2010).
- [15] Aubry, A., Lei, D. Y., Fernández-Domínguez, A. I., Sonnefraud, Y., Maier, S. A., Pendry, J. B., "Plasmonic Light-Harvesting Devices over the Whole Visible Spectrum," Nano Lett. 10(7), 2574–2579 (2010).
- [16] Thomann, I., Pinaud, B. A., Chen, Z., Clemens, B. M., Jaramillo, T. F., Brongersma, M. L., "Plasmon Enhanced Solar-to-Fuel Energy Conversion," Nano Lett. 11(8), 3440–3446 (2011).
- [17] Munday, J. N., Atwater, H. A., "Large Integrated Absorption Enhancement in Plasmonic Solar Cells by Combining Metallic Gratings and Antireflection Coatings," Nano Lett. 11(6), 2195–2201 (2011).
- [18] Yu, R., Lin, Q., Leung, S.-F.., Fan, Z., "Nanomaterials and nanostructures for efficient light absorption and photovoltaics," Nano Energy 1(1), 57–72 (2012).
- [19] Raschke, G., Kowarik, S., Franzl, T., Sönnichsen, C., Klar, T. A., Feldmann, J., Nichtl, A., Kürzinger, K., "Biomolecular Recognition Based on Single Gold Nanoparticle Light Scattering," Nano Lett. 3(7), 935–938 (2003).
- [20] Homola, J., "Present and future of surface plasmon resonance biosensors," Anal. Bioanal. Chem. 377(3), 528–539 (2003).
- [21] Jain, P. K., Huang, X., El-Sayed, I. H., El-Sayed, M. A., "Review of Some Interesting Surface Plasmon Resonance-enhanced Properties of Noble Metal Nanoparticles and Their Applications to Biosystems," Plasmonics 2(3), 107–118 (2007).
- [22] Anker, J. N., Hall, W. P., Lyandres, O., Shah, N. C., Zhao, J., Van Duyne, R. P., "Biosensing with plasmonic nanosensors," Nat. Mater. 7(6), 442–453 (2008).
- [23] Chung, T., Lee, S.-Y., Song, E. Y., Chun, H., Lee, B., "Plasmonic Nanostructures for Nano-Scale Bio-Sensing," Sensors 11(11), 10907–10929 (2011).
- [24] Brolo, A. G., "Plasmonics for future biosensors," Nat. Photonics 6(11), 709–713 (2012).

- [25] Sivanesan, A., Izake, E. L., Agoston, R., Ayoko, G. A., Sillence, M., "Reproducible and label-free biosensor for the selective extraction and rapid detection of proteins in biological fluids," J. Nanobiotechnology 13(1), 43 (2015).
- [26] Nusir, A. I., A. M. Hill, M. O. Manasreh, and J. B. Herzog. "Near-infrared metal-semiconductor-metal photodetector based on semi-insulating GaAs and interdigital electrodes." Photonics Research 3, no. 1 (2015): 1-4.
- [27] Ahmad A. Darweesh, Bauman, Stephen J., and Joseph B. Herzog. "Improved optical enhancement using double-width plasmonic gratings with nanogaps." Under Review", 2016.
- [28] Herzog, Joseph B., Mark W. Knight, Yajing Li, Kenneth M. Evans, Naomi J. Halas, and Douglas Natelson. "Dark plasmons in hot spot generation and polarization in interelectrode nanoscale junctions." Nano letters 13, no. 3: 1359-1364 (2013).
- [29] Herzog, Joseph B., Mark W. Knight, and Douglas Natelson. "Thermoplasmonics: quantifying plasmonic heating in single nanowires." Nano letters 14, no. 2: 499-503 (2014).
- [30] Saylor, Cameron, Eric Novak, Desalegn Debu, and Joseph B. Herzog. "Investigation of maximum optical enhancement in single gold nanowires and triple nanowire arrays." Journal of Nanophotonics 9, no. 1: 093053-093053 (2015).
- [31] Prodan, E., C. Radloff, Naomi J. Halas, and P. Nordlander. "A hybridization model for the plasmon response of complex nanostructures." Science 302, no. 5644: 419-422 (2003).
- [32] Nordlander, Peter, C. Oubre, E. Prodan, K. Li, and M. I. Stockman. "Plasmon hybridization in nanoparticle dimers." Nano letters 4, no. 5: 899-903 (2004).
- [33] Brandl, Daniel W., Chris Oubre, and Peter Nordlander. "Plasmon hybridization in nanoshell dimers." The Journal of chemical physics 123, no. 2: 024701 (2005).